Sustainable Energy & Fuels

PAPER

View Article Online
View Journal | View Issue

Cite this: *Sustainable Energy Fuels*, 2019, **3**, 272

Capture and conversion of carbon dioxide by solar heat localization†

Varun Kashyap,[a] Riddhiman Medhi,[b] Peyman Irajizad,[a] Parham Jafari,[a] Masoumeh Nazari,[a] Ali Masoudi,[a] Maria D. Marquez,[b] T. Randall Lee *[b] and Hadi Ghasemi *[a]

Received 8th November 2018
Accepted 12th November 2018

DOI: 10.1039/c8se00546j

rsc.li/sustainable-energy

As the world slowly transitions from conventional fossil fuels to renewable forms of energy, environmentally friendly CO_2 capture is urgently needed. Currently, liquid amine and ionic liquid-based systems are utilized for this purpose. However, these forms of capture mostly lead to the formation of stable carbamate salts with high enthalpy of formation, and it is therefore difficult to recover the initial liquid for cyclic operation. Furthermore, amine-based technologies pose concerns including toxic emissions and volatility, while ionic liquid-based systems suffer from complexity of liquid handling and high operational cost. Herein, we report a solid-state sustainable CO_2 collector (SCC), which is activated by solar heat localization. This stable cyclic SCC is based on ionic liquids and graphene aerogel, which undergoes solid–liquid phase change to efficiently capture and convert CO_2. The SCC captures 0.2 moles of CO_2 for every mole of ionic liquid and converts the absorbed CO_2 into useful byproducts, including water and calcium carbonate in each cycle. A system prototype of the SCC is developed and demonstrated. The SCC provides a new and promising paradigm to efficiently capture and convert CO_2 using abundant solar energy to address global emissions and consequent environmental challenges.

Introduction

Global CO_2 emissions have increased at an alarming rate of approximately 40% over the last 10 to 15 years,[1] with the rate expected to double by 2050.[2] As a consequence, the reduction of environmental CO_2 has major implications on the global society,[3] and its capture is being viewed as one of the most prominent means of decarbonization. Demands for efficient CO_2 capture technologies are driving the exploration of different mechanisms.[4] Current commercial technologies employed for CO_2 capture include the use of amine-based solvents, mainly monoethanolamine (MEA), diethanolamine, and methyldienthanolamine.[5–7] However, these forms of capture lead to the formation of stable carbamate/carbonate salts,[8] making it difficult to recover the amine-based solvent for cyclic operation. Furthermore, the large enthalpy of CO_2 capture reaction corresponds to highly energy intensive and costly cyclic systems.[9,10] Amine-based systems suffer from low CO_2 capture capacity,[10] toxicity,[11] loss of reagent due to evaporation, and equipment corrosion.[12] To address these drawbacks, ionic liquids (ILs) are being considered as an alternative for CO_2 capture systems.

Ionic liquids, which are salts with melting points below 100 °C,[10] have gained attention in various fields due to their tunable molecular structures,[13] ILs enjoy unique properties such as low volatility, nonflammability, high thermal stability, and high CO_2 solubility.[14,15] The aforementioned properties have made ILs a desirable alternative to conventional methods of CO_2 capture.[16,17] Various imidazolium anion-based ILs have been studied, mainly in the liquid state for CO_2 capture involving both physisorption and chemisorption.[10] In physisorption, the CO_2 molecules occupy the intermolecular spaces of the ILs without forming any chemical bonds. Molecular interactions (mainly van der Waals forces) between the CO_2 and IL molecules, primarily the anionic part, is the mechanism behind the capture.[18] In chemisorption, which is also studied for functionalized cations and anions,[19,20] chemical reactions take place between the imidazolium nitrogen and CO_2, mainly leading to the formation of carbamate salts. Similar to most amine-based technologies, to reuse ILs after a chemical reaction, it is required to reverse the CO_2 absorption and carbamate formation steps, making the process energy intensive and costly. Furthermore, irrespective of the type of absorption, ILs are mainly used in the liquid state, which adds additional complexities including fluid lines, pumps, and other operational structures. As a result, research has been devoted to find methods for efficient and cyclic CO_2 capture in the form of

[a]Department of Mechanical Engineering, University of Houston, Houston, TX 77204-4006, USA. E-mail: hghasemi@uh.edu

[b]Department of Chemistry and the Texas Center for Superconductivity, University of Houston, Houston, TX 77204-5003, USA. E-mail: trlee@uh.edu

† Electronic supplementary information (ESI) available. See DOI: 10.1039/c8se00546j

solid-state material structures. In this study, a new solid-state approach and the related material paradigm called "sustainable CO_2 collector" (SCC), illustrated in Fig. 1, is proposed for CO_2 capture and conversion. This approach is cyclic, scalable, energy efficient, and non-toxic. The process also produces beneficial calcium carbonate, which is used in water treatment, manufacturing of cement, plaster, and mortars.[21] The SCC structure is comprised of ILs incorporated in a graphene aerogel matrix. To develop a stable material structure, the IL in the SCC exists in the solid state. However, CO_2 capture capacity for ILs in the liquid state is higher than that in the solid state. To stimulate solid–liquid phase change, we utilize the concept of solar heat localization. Neumann *et al.*[22] and Ghasemi *et al.*[23] introduced the concept of heat localization at the liquid–vapor interface for solar steam generation. Here, the material structure concentrates the thermal energy (provided by solar irradiation) needed for phase change while minimizing energy losses. Plasmonic nanoparticles and carbon-based material structures were studied to implement this concept.[24–26] For heat localization, the material matrix must possess the following properties: high volumetric absorption in the solar spectrum and low thermal conductivity to localize thermal energy. In addition to heat localization for solid–liquid phase change, the material should contain the ionic liquid for CO_2 capture. Therefore, the material must possess high permeability to hold large volumes of the ionic liquid, hydrophobicity to avoid the retention of water in the material matrix, and oleophilicity to wet and retain the ionic liquid. Therefore, graphene aerogels were used for the SCC material matrix. Steps 1 and 2 in Fig. 1 show the IL integrated within the graphene aerogel. The process of integration is presented in the ESI.† Due to heat localization, a temperature above the melting point of the IL is reached within the graphene aerogel, thereby facilitating solid–liquid phase change in the IL. In Step 3, CO_2 gas is passed through the SCC for absorption. Once the SCC absorbs the CO_2 and is no longer exposed to solar irradiation, the IL in the SCC goes back to its solid state as shown in Step 4. In Step 5, the SCC is washed with dilute (0.01 M) $Ca(OH)_2$ solution. The absorbed CO_2 in the IL reacts with this solution to form $Ca(HCO_3)_2$ filtrate. The $Ca(HCO_3)_2$ precipitates out as $CaCO_3$ in Step 6, thereby leaving behind pure water. We emphasize that this cycle is repeatable, and the same SCC can be used to continuously capture CO_2 and precipitate $CaCO_3$ as the byproduct. A prototype has been developed to demonstrate the continuous operation of the SCC and is described in the ESI (Fig. S9†). Note that the price of precipitated $CaCO_3$ is ~$7/kg more than $Ca(OH)_2$ and is also used in a wide range of industries.

Results and discussion

Heat localization, effect of phase change, and selection of ILs

Fig. 2 shows the effect of phase change on CO_2 capture in the SCC. To initiate the solid–liquid phase change, graphene

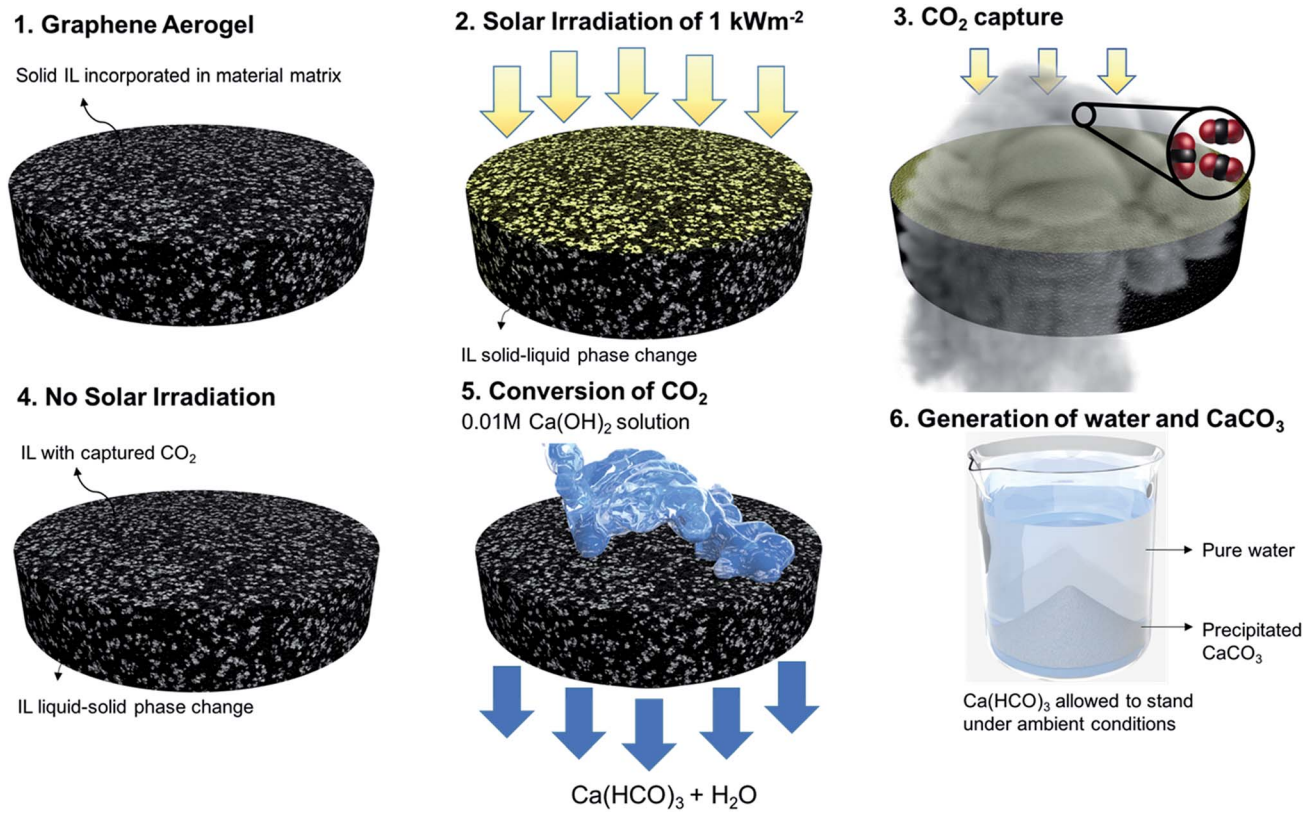

Fig. 1 Cyclic CO_2 capture and its subsequent conversion to water and $CaCO_3$. Steps 1 and 2 illustrate the structure of the SCC and the solid–liquid phase change initiated by heat localization. Steps 3 and 4 show the capture of CO_2 into the SCC. Steps 5 and 6 illustrate the washing and subsequent precipitation of $CaCO_3$. (A video on prototype of this cyclic SCC is shown in Movie S1†).

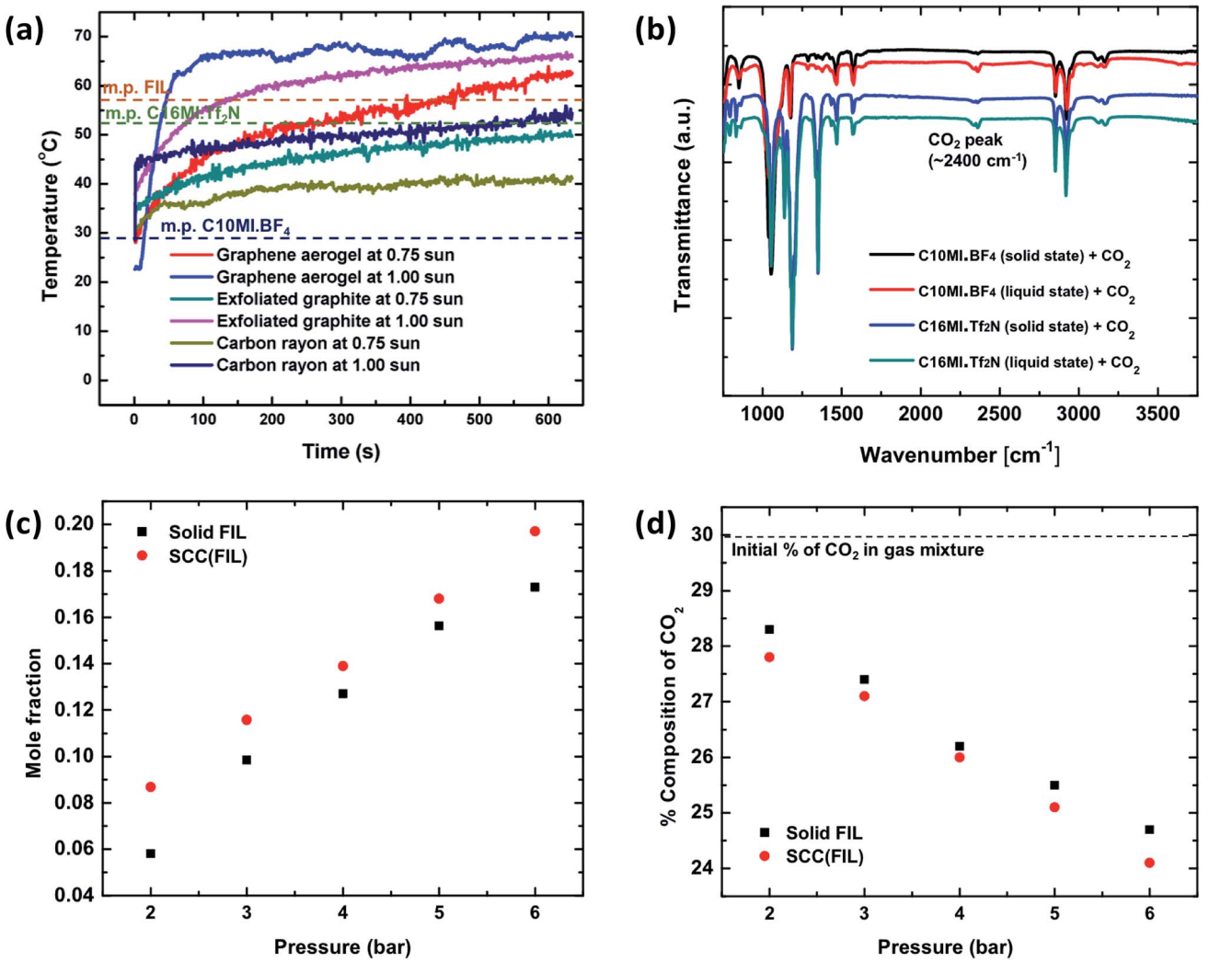

Fig. 2 The effect of phase change on CO_2 capture in ionic liquids is shown. (a) To initiate solid–liquid phase change, the concept of heat localization is used. Maximum temperature achieved by different materials at 1 sun and 0.75 sun solar illumination is shown. (b) FTIR measurements are conducted to evaluate capture of CO_2 in solid and liquid states, the average of two trials for each spectrum is reported here. (c) A plot of mole fraction of absorbed CO_2 as a function of pressure is shown. The SCC with the liquid-state ionic liquid shows higher capture compared to the SCC with the solid-state ionic liquid. (d) Percentage drop in CO_2 concentration is plotted as a function of pressure.

aerogel is used for heat localization. Graphene aerogel was synthesized to serve as the matrix material following a previously reported method;[27] synthetic details are provided in the ESI.† An optical image of the graphene aerogel is shown in Fig. S1.† To evaluate solar heat localization of the graphene aerogel, we measured its temperature as a function of time under solar irradiation of 1 kW m^{-2} and 0.75 kW m^{-2}. Furthermore, we compared its solar heat localization with other materials including exfoliated graphite and carbonized rayon. A previously developed experimental setup was used to minimize side heat losses.[28] Fig. 2a shows the temperature increase as a function of time for these materials under 1 kW m^{-2} and 0.75 kW m^{-2} solar irradiation. As shown in the figure, the graphene aerogel at 1 sun solar irradiation reaches a higher temperature (~70 °C) in comparison to exfoliated graphite and carbon rayon. This provides a wider melting point temperature range for the selection of ILs for the SCC. We therefore chose graphene aerogel as the material matrix to hold the ionic liquid in the SCC.

The ILs chosen to be incorporated in graphene aerogel must have a melting point between 30 and 70 °C in order to show solid–liquid phase change under 1 kW m^{-2} solar illumination and must contain imidazolium-based cations with high molecular weights and fluorinated anions for enhanced CO_2 absorption.[18] It is also desired to have ILs largely immiscible in water to avoid loss of ILs during the washing process with $Ca(OH)_2$ solution. Miscibility of ILs in water depends on the water-ion interaction strength, degree of fluorination, size of ions (larger fluorinated ions are less miscible) and magnitude of the localized charge in the connecting atom.[29] Based on the above properties, two commercial ionic liquids were chosen, C10MI.BF_4 and C16MI.Tf_2N. The structures of these ionic liquids are shown in Fig. S2.† In addition to commercially available ionic liquids, we demonstrated CO_2 capture in ionic

liquids with fluorinated cation groups. Fluorination of the cation can significantly improve the CO_2 solubility, although to a lesser extent than anion fluorination.[30] Fluorination of ionic liquids makes them more selective toward CO_2 absorption compared to alkyl chain cations.[31] Thus, to achieve enhanced CO_2 absorption in our system, we synthesized and utilized an imidazolium ionic liquid having more extensive fluorination than C10MI.BF_4 and C16MI.Tf_2N, $[CF_3(CF_2)_7(CH_2)_3MI][(CF_3CF_2SO_2)_2N]$, henceforth abbreviated simply as fluorinated ionic liquid (FIL). The synthesis procedure is discussed in the ESI,† and NMR confirmation of the product is provided in Fig. S3.† This ionic liquid has a reported melting point of 56 °C.[32] Note that SCC (X) is the general nomenclature used to represent a SCC composed from a specific IL – X, and so forth.

To study absorption of CO_2 in ILs in the solid and liquid states, we conducted three different experiments: FT-IR, mole fractions of captured CO_2, and percentage change in CO_2 composition in the CO_2–nitrogen mixture using the gas analyzer. Fig. 2b shows the FT-IR spectra for C10MI.BF_4 and C16MI.Tf_2N ILs in the solid and liquid states. As shown, the intensity of the peak for CO_2 in the liquid sample is significantly higher than that in the solid state. Two separate experimental setups were developed, as described in the ESI (illustrated in Fig. S4 and S5†) to quantify the amount of CO_2 captured by the SCC (FIL) with the FIL in the liquid state and in the solid state. In the first experiment, the pressure in the cylindrical high-pressure chamber was maintained between 2 bar and 6 bar for ~40 minutes. The mole fraction of CO_2 captured is shown in Fig. 2c. As shown, there is a difference of ~18–50% in CO_2 capture between FIL and SCC (FIL) depending on the CO_2 pressure, suggesting higher capture in the liquid state than that in the solid state. In the second experiment, the change in the percentage composition of CO_2 was measured in the CO_2–nitrogen mixture using the gas analyzer. Nitrogen is used in the gas mixture to demonstrate the selective absorption of the SCC toward CO_2. As shown in Fig. 2d, the change in the CO_2

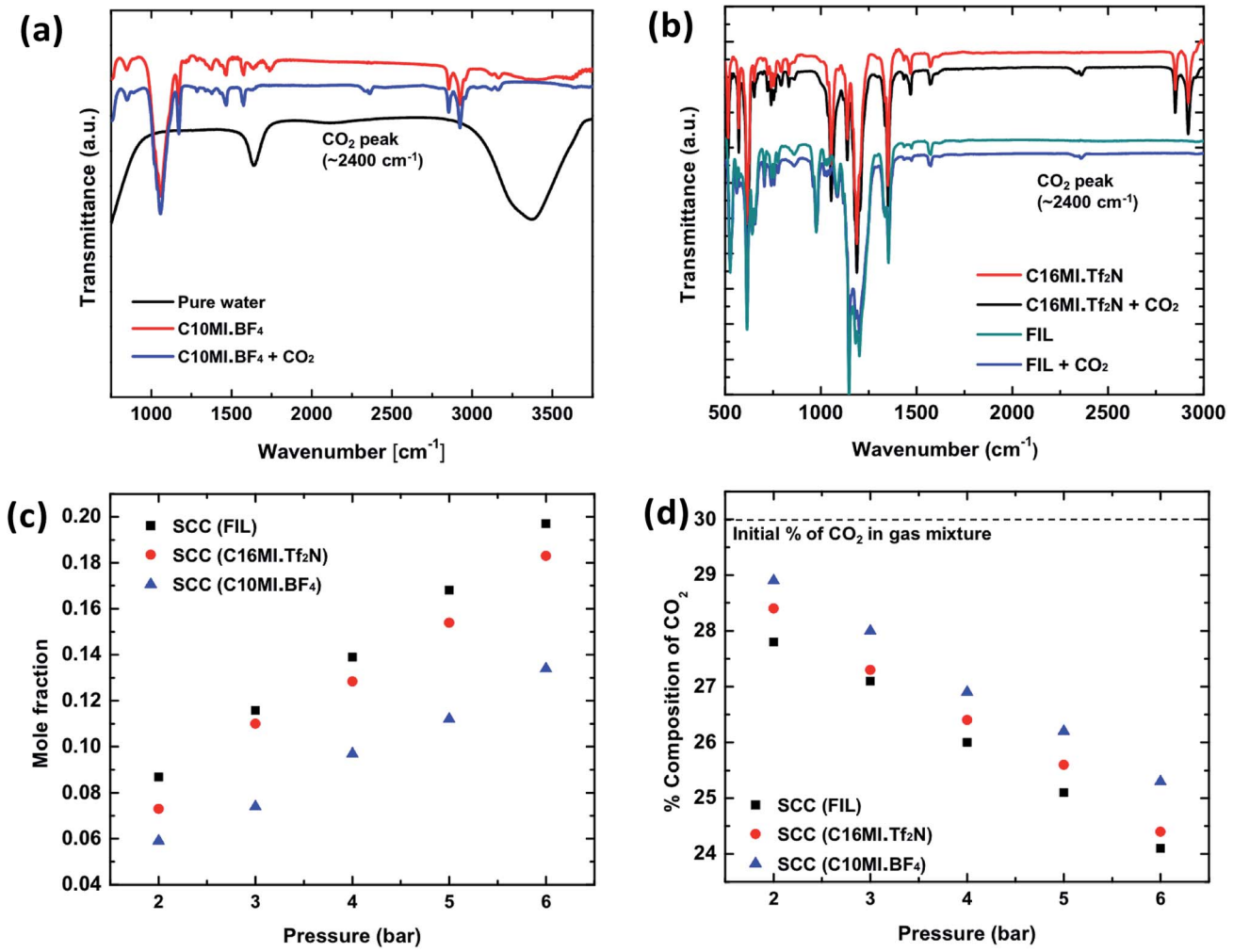

Fig. 3 CO_2 capture in the SCCs using various ionic liquids is shown. The effect of fluorination of the cation is demonstrated in these graphs. (a) FT-IR spectrum for the capture of CO_2 using C10MI.BF_4 ionic liquid. The presented FT-IR spectra are representative of 2 sets of measurements. Note that atmospheric CO_2 was purged out to ensure its absence from the spectra. (b) FT-IR spectrum for the CO_2 capture in C16MI.Tf_2N and FIL are shown. (c) Pressure drop experiments were conducted using a high-pressure chamber to quantify the CO_2 capture in terms of mole fraction. (d) Change in percentage of CO_2 was quantified using a gas analyzer.

concentration is higher for SCC (FIL) in the liquid state, thereby indicating higher capture compared to FIL (solid state). Note that the percentage of nitrogen remains constant in the mixture. In Fig. 2d, we have studied a mixture of gases (N_2 and CO_2), but in Fig. 2c, we have analyzed the SCC under pure CO_2. Depending on the application, both scenarios might occur.

CO_2 capture using the sustainable CO_2 collector (SCCs)

CO_2 absorption in the chosen ILs was quantified initially using a FT-IR method. Fig. 3a and b show the FT-IR spectra for ILs C10MI.BF_4, C16MI.Tf_2N, and FIL after CO_2 absorption, wherein a clear peak for CO_2 is seen at 2400 cm^{-1}, in accordance with earlier reports of CO_2 FT-IR measurements.[33] To confirm that the peak is not due to atmospheric CO_2, IR measurements were conducted after purging the compartment with nitrogen gas to remove atmospheric CO_2. The IR spectrum of pure water was also obtained. Multiple trials consistently revealed a CO_2 peak for the IL samples only, verifying the capture of CO_2. No changes were observed in the base IL patterns, thereby indicating that the CO_2 is absorbed in the ILs *via* physisorption. Furthermore, analysis of solid C16MI.Tf_2N by ^{13}C NMR spectroscopy indicates CO_2 absorption as shown in Fig. S6 and S7.†

Experimental setups similar to the ones described in the previous section (Fig. S4 and S5†) were also used to quantify CO_2 capture in the SCC with the chosen ILs. Fig. 3c shows the mole fraction of CO_2 captured as a function of pressure. These experiments were conducted for the SCC (C16MI.Tf_2N), SCC (C10MI.BF_4), and SCC (FIL) samples. Solar irradiation of 1 sun was incident on the sample to stimulate solid–liquid phase change. The mole fraction of CO_2 captured is comparable to values reported in earlier literature for ILs.[18] As shown, the capture in SCC (FIL) is slightly higher than SCC (C16MI.Tf_2N) due probably to the higher degree of fluorination in the former IL. Fig. 3d shows the percentage drop of CO_2 as a function of

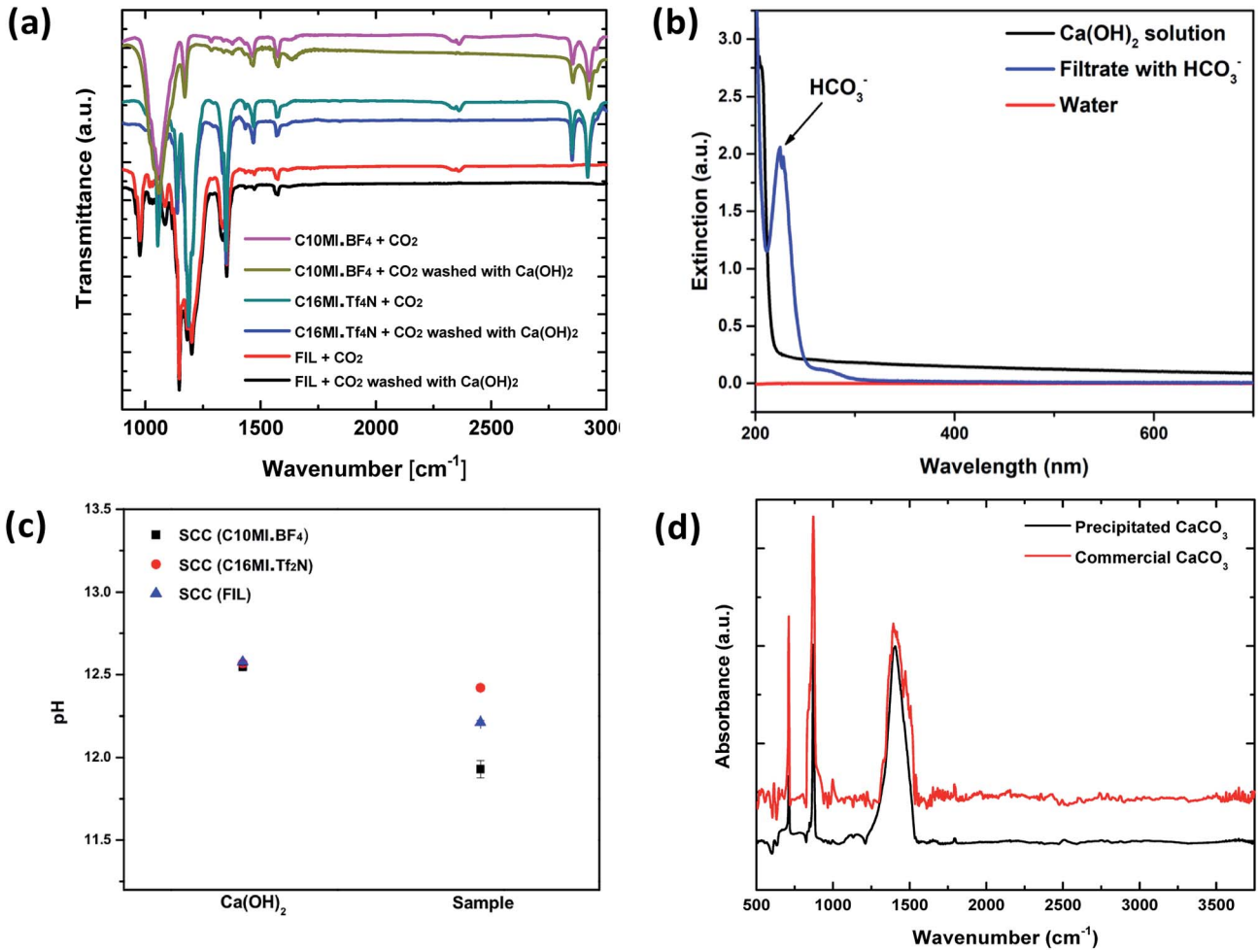

Fig. 4 Verification of the conversion of CO_2 to calcium bicarbonate and subsequently to $CaCO_3$. (a) FT-IR spectrum to verify CO_2 present before and after washing with $Ca(OH)_2$ is shown. On washing with $Ca(OH)_2$, the CO_2 peak at ~2400 cm^{-1} disappears, thereby confirming the reaction of the absorbed CO_2 with the $Ca(OH)_2$. (b) UV-vis spectrum is shown for the $Ca(OH)_2$ solution used for washing and for the filtrate formed after washing. The presence of $Ca(HCO_3)_2$ in the filtrate is shown. Note that this UV-vis spectrum is taken as soon as the SCC is washed. (c) pH measurements were conducted to verify the formation of $Ca(HCO_3)_2$ in the filtrate on washing with $Ca(OH)_2$. A constant drop in pH can be seen in the filtrate. Note that these points are averaged over three trials. (d) FTIR spectrum for the final precipitated $CaCO_3$ is shown. This is in good agreement with the standard spectrum for $CaCO_3$.

pressure for SCC (C16MI.Tf_2N), SCC (C10MI.BF_4), and SCC (FIL). As shown in the figure, the maximum drop in percentage of CO_2 in the gas mixture is observed for SCC (FIL). This trend is consistent with the mole fraction of CO_2 captured for these ILs. The gas analyzer results confirm the absorption selectivity for CO_2 over N_2 as predicted based on previous studies.[10] Therefore, the selective capture of CO_2 in SCCs is confirmed from these experiments.

Conversion of the absorbed CO_2 to soluble HCO_3^-

The chemical reactions involved in the reuse of the SCC for multiple cycles and conversion of the absorbed CO_2 to precipitated calcium carbonate are described in the ESI.† The reaction of calcium hydroxide with CO_2 to form calcium carbonate and calcium bicarbonate is well known.[34] $Ca(OH)_2$, commonly called "slaked lime", primarily produces $CaCO_3$ but forms $Ca(HCO_3)_2$ in the presence of excess CO_2.[35] Both of these reactions are spontaneous.[34]

Solutions having low concentrations of $Ca(OH)_2$ in combination with an excess of CO_2 selectively form the soluble $Ca(HCO_3)_2$ species that is washed from the SCC. Fig. 4 shows the process of washing the SCC with $Ca(OH)_2$ to obtain precipitated $CaCO_3$. The absorption of CO_2 into a $Ca(OH)_2$ solution is more efficient if the concentration of $Ca(OH)_2$ is low.[10] This is because lower concentrations of $Ca(OH)_2$ lead to CO_2 absorbed in the solution, forming a mixture of mainly soluble bicarbonate ions.[34] We used a 0.01 M $Ca(OH)_2$ solution to wash the CO_2 out of SCC (FIL). SCC (FIL), being mostly immiscible in water, remains unchanged, while the CO_2 is converted to the soluble HCO_3^- species and is collected in the filtrate. Fig. 4a shows the FT-IR spectra for the disappearance of the CO_2 peak at ~2400 cm^{-1} after washing the ILs with this $Ca(OH)_2$ solution, confirming the effectiveness of the washing process.

Conversion of the CO_2 to soluble HCO_3^- is confirmed by its presence in the filtrate *via* UV-vis spectroscopy, as shown in Fig. 4b. Note that the UV-vis spectrum was obtained soon after the SCC was washed with the $Ca(OH)_2$ solution. From these observations, the presence of $Ca(HCO_3)_2$ in the filtrate can be confirmed, implying effective washing of the SCC and conversion of the absorbed CO_2. We then used an electronic pH meter (Mettler Toledo) with a measuring probe to compare the pH levels between the calcium hydroxide solution before and after washing the CO_2-impregnated SCCs. The experiment was conducted for the SCC containing all three different ionic liquids (C10MI.BF_4, C16MI.Tf_2N, and FIL) for three trials to confirm the reproducibility of the results. A drop in the pH was observed in the filtrate compared to the starting $Ca(OH)_2$ solution used for washing the ionic liquid, as shown in Fig. 4c. This experiment thus implicates the consumption of OH^- to form the less basic HCO_3^- species in solution, responsible for the drop in pH.[36]

Final conversion to precipitated $CaCO_3$ and reusability of the SCC

Soluble HCO_3^- is benign, but it is not the most commercially useful form of carbonate species. A conversion to a more useful product is desired. Precipitated $CaCO_3$ enjoys widespread use in a variety of industries, including paints, plastics, papers, and sealants.[21] Therefore, to precipitate $CaCO_3$ from $Ca(HCO_3)_2$ solution, the solution was left to stand as reported by earlier studies.[37] Once the excess CO_2 escapes from the solution, precipitated $CaCO_3$ is left behind, which was verified by the FT-IR spectrum shown in Fig. 4d. The spectrum shows pure $CaCO_3$ as compared to reference spectrum of commercial $CaCO_3$. Although in both cases of SCC (C16MI.Tf_2N) and SCC (FIL), we recovered pure $CaCO_3$, in the case of SCC (C10MI.BF_4), due to the low solubility of BF_4 anions in the water, we detected residual IL, as indicated by the C–H stretching peaks in the FT-IR spectrum in Fig. S10.† Another method to precipitate calcium carbonate is to treat the bicarbonate filtrate with excess $Ca(OH)_2$ solution, which will precipitate out the calcium as calcium carbonate, as per eqn (3) in the ESI.† Optical images for

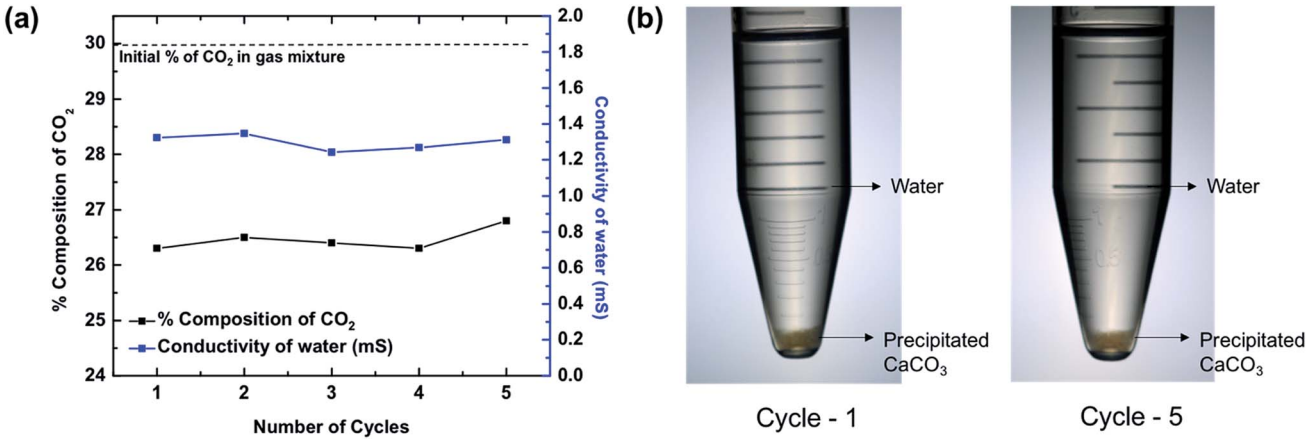

Fig. 5 The SCC is tested for repeatability over five cycles. (a) SCC (FIL) is used to capture CO_2, and the final percentage composition of CO_2 is measured over five cycles. At ~4 bar pressure, a nearly constant drop in the percentage of CO_2 is observed in the gas mixture over multiple trials, thereby confirming the repeatability of the SCC. (b) Optical images of the byproducts including precipitated $CaCO_3$ and water are shown for Cycle-1 and Cycle-5.

the products of this reaction are shown in Fig. S8.† The final byproducts obtained from the SCC are $CaCO_3$ and water. Note that the number of moles of H_2O formed is equal to the number of moles of CO_2 absorbed.

To confirm the reusability of the SCCs, repeated CO_2 absorption and washing over multiple cycles were conducted on SCC (FIL), since this proved to be the most efficient material based on the previous experiments. The gas analyzer set up and protocol (Fig. S5†) was used to evaluate the reusability of the SCC. Fig. 5a shows the plot of percentage composition of CO_2 in the resulting mixture as a function of repetition for 4 bar operating pressure. We found that the percentage composition of the final mixture remains constant even after 5 cycles, thereby demonstrating the excellent reusability of the SCCs. Fig. 5a shows the conductivity of water obtained from the reaction after the precipitation of $CaCO_3$. Similar conductivity is observed over five cycles as seen from the graph. Optical images of the byproducts including precipitated $CaCO_3$ and water for the 1st and 5th cycles are shown in Fig. 5b. Furthermore, we should emphasize that the price of precipitated $CaCO_3$ is ~$7/kg more than $Ca(OH)_2$, which is the initial constituent of the reaction.

Conclusions

In conclusion, we have developed a concept and corresponding material paradigm for reusable CO_2 capture while forming extremely useful precipitated $CaCO_3$. Precipitated calcium carbonate has multiple applications including the manufacture of paints, plastics, papers, and sealants. Furthermore, the concept of heat localization with a graphene aerogel matrix was utilized to stimulate solid–liquid phase change, thereby increasing the CO_2 capture capacity. The use of solar energy further reduces the energy cost requirements for large scale implementation. We envision our SCC to be used for CO_2 capture during flue gas emission and the natural gas sweetening process. CO_2 capture in these applications will directly affect CO_2 concentration in the atmosphere. The next step for the implementation of this concept is to test the SCC in high pressure flue gas emission sites. We believe this concept and corresponding technology will assist in a smooth transition toward renewable energy sources.

Conflicts of interest

A provisional patent is filed with application number 62624333 in USPTO.

Acknowledgements

The authors gratefully acknowledge funding support from the Air Force Office of Scientific Research (Grant AFOSR FA9550-16-1-0248, H. G.) with Dr Ali Sayir as program manager, Air Force Office of Scientific Research (Grant AFOSR FA9550-18-1-0094, T. R. L.), the Robert A. Welch Foundation (E-1320, T. R. L.) and the Texas Center for Superconductivity at the University of Houston (TcSUH, T. R. L.). They thank Dr Jiming Bao of the University of Houston for help with FTIR measurements, Dr Scott Smith for help with NMR measurements, and Abdullah Al-Bayati and Carlin Ashford for help with synthesis of graphene aerogels.

References

1 IEA, *CO_2 emissions from fuel combustion: Highlights. Outlook*, 2010, vol. 38, pp. 1–134.
2 International Energy Agency, *Energy Technology Perspectives: Scenarios & Strategies To 2050*, 2010.
3 IPCC, *Climate Change 2007 Synthesis Report*, 2007.
4 A. D. Ritter and J. A. Ebner, *Sep. Sci. Technol.*, 2009, **44**, 1273–1421.
5 J. D. Figueroa, T. Fout, S. Plasynski, H. McIlvried and R. D. Srivastava, *Int. J. Greenhouse Gas Control*, 2008, **2**, 9–20.
6 G. T. Rochelle, *Science*, 2009, **325**, 1652–1654.
7 B. Dutcher, M. Fan and A. G. Russell, *ACS Appl. Mater. Interfaces*, 2015, **7**, 2137–2148.
8 P. D. Vaidya and E. Y. Kenig, *Chem. Eng. Technol.*, 2007, **30**, 1467–1474.
9 O. F. Dawodu and A. Meisen, *Can. J. Chem. Eng.*, 1996, **74**, 960–966.
10 M. Ramdin, T. W. De Loos and T. J. H. Vlugt, *Ind. Eng. Chem. Res.*, 2012, **51**, 8149–8177.
11 D. M. D'Alessandro, B. Smit and J. R. Long, *Angew. Chem., Int. Ed.*, 2010, **49**, 6058–6082.
12 R. Davidson, *Clean Coal Cent.*, 2007, vol. 125.
13 S. Zhang, N. Sun, X. He, X. Lu and X. Zhang, *J. Phys. Chem.*, 2006, **35**, 1475–1517.
14 X. X. Zhang, X. X. Zhang, H. Dong, Z. Zhao, S. Zhang and Y. Huang, *Energy Environ. Sci.*, 2012, **5**, 6668.
15 J. F. Brennecke and B. E. Gurkan, *J. Phys. Chem. Lett.*, 2010, **1**, 3459–3464.
16 J. E. Bara, S. Lessmann, C. J. Gabriel, E. S. Hatakeyama, R. D. Noble and D. L. Gin, *Ind. Eng. Chem. Res.*, 2007, **46**, 5397–5404.
17 B. A. Voss, J. E. Bara, D. L. Gin and R. D. Noble, *Chem. Mater.*, 2009, **21**, 3027–3029.
18 C. Cadena, J. L. Anthony, J. K. Shah, T. I. Morrow, J. F. Brennecke and E. J. Maginn, *J. Am. Chem. Soc.*, 2004, **126**, 5300–5308.
19 E. D. Bates, R. D. Mayton, I. Ntai and J. H. Davis, *J. Am. Chem. Soc.*, 2002, **124**, 926–927.
20 B. E. Gurkan, J. C. de la Fuente, E. M. Mindrup, L. E. Ficke, B. F. Goodrich, E. A. Price, W. F. Schneider and J. F. Brennecke, *J. Am. Chem. Soc.*, 2010, **132**, 2116–2117.
21 O. A. Jimoh, K. S. Ariffin, H. Bin Hussin and A. E. Temitope, *Carbonates Evaporites*, 2017, 1–16.
22 O. Neumann, A. S. Urban, J. Day, S. Lal, P. Nordlander and N. J. Halas, *ACS Nano*, 2013, **7**, 42–49.
23 H. Ghasemi, G. Ni, A. M. Marconnet, J. Loomis, S. Yerci, N. Miljkovic and G. Chen, *Nat. Commun.*, 2014, **5**, 4449.
24 G. W. Ni, S. H. Zandavi, S. M. Javid, S. V. Boriskina, T. A. Cooper and G. Chen, *Energy Environ. Sci.*, 2018, **1**, 1510–1519.
25 H. Song, Y. Liu, Z. Liu, M. H. Singer, C. Li, A. R. Cheney, D. Ji, L. Zhou, N. Zhang, X. Zeng, Z. Bei, Z. Yu, S. Jiang and Q. Gan, *Adv. Sci.*, 2018, 1800222.

26 J. Yang, Y. Pang, W. Huang, S. K. Shaw, J. Schiffbauer, M. A. Pillers, X. Mu, S. Luo, T. Zhang, Y. Huang, G. Li, S. Ptasinska, M. Lieberman and T. Luo, *ACS Nano*, 2017, **11**, 5510–5518.
27 L. M. Xu, G. Y. Xiao, C. B. Chen, R. Li, Y. Y. Mai, G. M. Sun and D. Y. Yan, *J. Mater. Chem. A*, 2015, **3**, 7498–7504.
28 V. Kashyap, A. Al-Bayati, S. M. Sajadi, P. Irajizad, S. H. Wang and H. Ghasemi, *J. Mater. Chem. A*, 2017, **5**, 15227–15234.
29 M. Klahn, C. Stüber, A. Seduraman and P. Wu, *J. Phys. Chem. B*, 2010, **114**, 2856–2868.
30 D. Almantariotis, T. Gefflaut, A. A. H. Pádua, J. Y. Coxam and M. F. Costa Gomes, *J. Phys. Chem. B*, 2010, **114**, 3608–3617.
31 D. Almantariotis, A. S. Pensado, H. Q. N. Gunaratne, C. Hardacre, A. A. H. Pádua, J.-Y. Coxam and M. F. Costa Gomes, *J. Phys. Chem. B*, 2017, **121**, 426–436.
32 H. Ma, B. Chu and B. S. Hsiao, *Eur. Polym. J.*, 2017, **87**, 398–405.
33 S. U. Rege and R. T. Yang, *Chem. Eng. Sci.*, 2001, **56**, 3781–3796.
34 S.-J. Han, M. Yoo, D.-W. Kim and J.-H. Wee, *Energy Fuels*, 2011, **25**, 3825–3834.
35 a M. Kalinkin, E. V Kalinkina, O. a Zalkind and T. I. Makarova, *Inorg. Mater.*, 2005, **41**, 1073–1079.
36 Y. G. Bodlaender, *Angew. Chem., Int. Ed.*, 1901, **14**, 381–390.
37 Y. Kitano, *Bull. Chem. Soc. Jpn.*, 1962, **35**, 1973–1980.